

High-Frequency Percussive Ventilation: Pneumotachograph Validation and Tidal Volume Analysis

Patrick F Allan MD

INTRODUCTION: High-frequency percussive ventilation (HFPV) is an increasingly used mode of mechanical ventilation, for which there is no proven real-time means of measuring delivered tidal volume (V_T). **OBJECTIVE:** To validate a pneumotachograph for HFPV and then exploit flow-sensor data to describe the behavior of both low-frequency and high-frequency breaths. **METHODS:** Sensor performance was gauged during changes in high-frequency (4–12 Hz) and low-frequency rate and ratio, mean airway pressure, oxygen concentration, heated or heated-humidified gas flow, and endotracheal tube diameter. Glass bottle (adiabatic V_T) and test lung (adiabatically derived low-frequency V_T) based adiabatic conditions provided both an initial source for analog-signal calibration and an accepted standard comparator to flow-sensor measurement of high-frequency and low-frequency (flow-sensor-derived) V_T , respectively. **RESULTS:** Pneumotachography proved accurate and precise over an array of tested settings and conditions when analyzing both high-frequency (difference between mean \pm SD high-frequency V_T and adiabatic V_T was $-0.2 \pm 1.8\%$, 95% confidence interval -0.5 to 0.9%) and low-frequency breaths (mean \pm SD difference between flow-sensor-derived low-frequency V_T and adiabatically derived low-frequency V_T was $0.6 \pm 2.4\%$, 95% confidence interval 0.1 – 1.1%). High-frequency V_T and frequency exhibited an exponential relationship. During HFPV, flow-sensor-derived low-frequency V_T had a mean \pm SD of $1,337 \pm 700$ mL, 95% confidence interval $1,175$ – $1,499$ mL. **CONCLUSIONS:** Readily available pneumotachography provided accurate measurements of low-frequency and high-frequency V_T during HFPV. In the setting of acute lung injury, typical HFPV settings may deliver injurious V_T . *Key words:* high-frequency percussive ventilation; HFPV; mechanical ventilation; tidal volume; V_T ; pneumotachography. [Respir Care 2010;55(6):734–740]

Introduction

Clinical application of high-frequency percussive ventilation (HFPV) in the setting of acute lung injury (ALI) and smoke inhalation has led to consistent improvements in gas exchange.^{1–11} HFPV employs a singular high-

frequency flow to create a pressure-limited, time-cycled, “low-frequency” tidal volume (V_T) breath similar to that used in conventional mechanical ventilation (Fig. 1). However, neither the low-frequency nor the high-frequency volumes administered by HFPV are measured by the ventilator’s pressure transducers.

Importantly, contemporary mechanical ventilation strategies specific to ALI dictate that V_T be confined to within 4–8 mL/kg ideal body weight.^{12,13} It follows that our inability to ascertain V_T magnitude could result in clinicians unknowingly inflicting a form of ventilator-induced lung injury known as volutrauma. We therefore developed an HFPV-specific flow sensor to quantify V_T and reduce the risk of ventilator-induced lung injury.^{14–21}

For the purposes of this study, both pneumotachography and heated-wire flow sensors have consistently demonstrated the best accuracy and precision in measuring high-frequency V_T .^{18–21} To the best of our knowledge, only

Patrick F Allan MD is affiliated with the Pulmonary Medicine Service, Landstuhl Regional Medical Center, Landstuhl, Germany.

The opinions and assertions in this paper are the private views of the author and are not to be construed as reflecting the views of the United States Department of the Air Force or the Department of Defense.

The author has disclosed no conflicts of interest.

Correspondence: Patrick F Allan MD, Pulmonary Medicine Service, Landstuhl Regional Medical Center, CMR 402, Box 307, APO AE 09180, Landstuhl, Germany. E-mail: patrick.allan@amedd.army.mil.

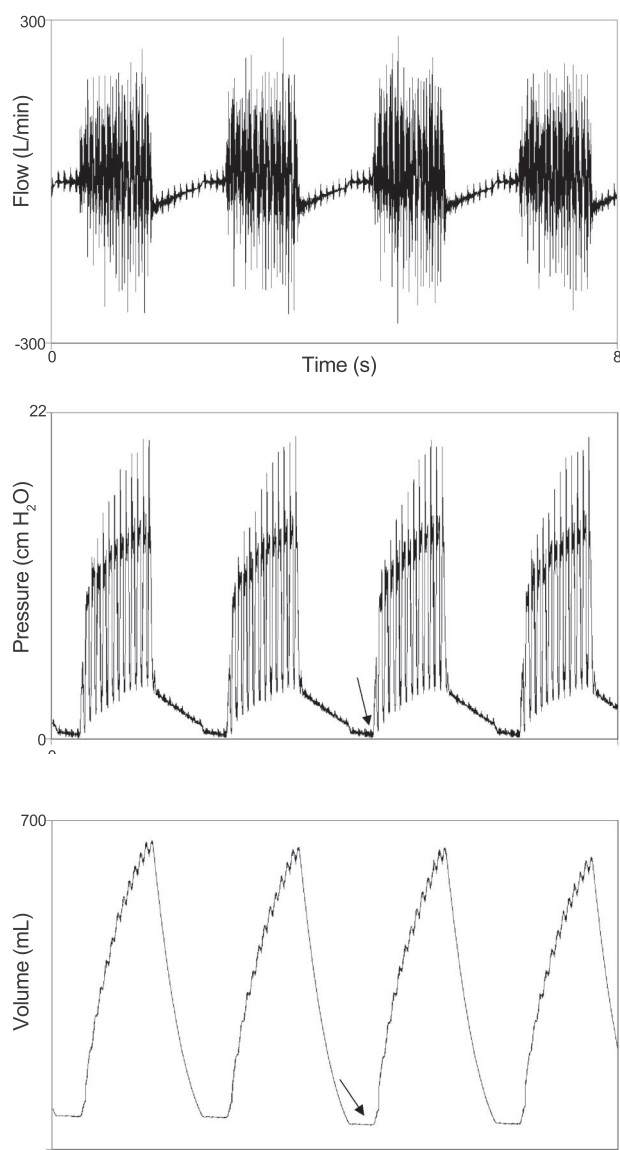


Fig. 1. Eight-second graph of high-frequency flow, high-frequency pressure, and low-frequency tidal volume. The graphs demonstrate an accumulation in high-frequency flow and pressure over the duration of a set inspiratory time to achieve a low-frequency tidal volume and flow. The end-expiration point is indicated by the arrow.

pneumotachograph sensors have received FDA approval for clinical use. Because of the projected appeal for such a device in other HFPV-equipped facilities, this exploration was limited to a readily accessible FDA-approved candidate.

Pneumotachograph readings were first assessed for accuracy and precision, using an *in vitro* validation construct. Once validated, the respective flow-sensor data were also exploited to describe high-frequency and low-

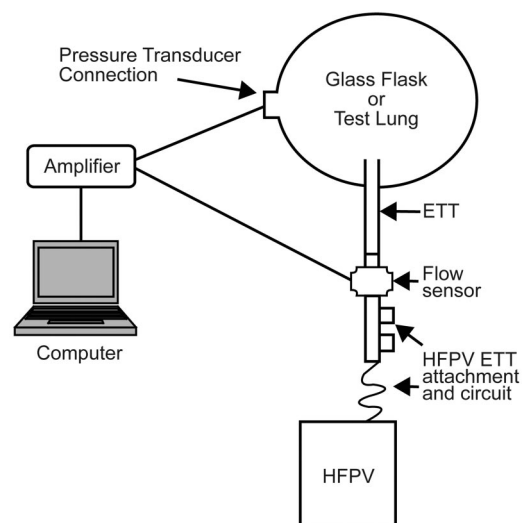


Fig. 2. Simplified schematic of the ventilator, flow sensor, and test-lung setup. Adiabatic tidal volume (V_T) was calculated as flask/lung Δ pressure. Flow-sensor V_T was calculated via analog signal integration. HFPV = high-frequency percussive ventilator. ETT = endotracheal tube.

frequency V_T behavior across a series of ventilator settings and gas flow conditions. This study represents part of an ongoing series of *in vitro* investigations probing the merits and deficiencies of HFPV.²²⁻²⁴

Methods

Ventilator and Glass Flask Setup: High-Frequency Tidal Volume Measurement

A high-frequency percussive ventilator (Volumetric Diffusive Respirator [VDR-4], Percussionaire, Sandpoint, Idaho) was connected in series with the flow sensor, an 8.0-mm cuffed endotracheal tube (ETT) (Hi-Lo, Mallinckrodt, Hazelwood, Missouri), and a 6-L glass flask. Total system compliance (ETT and glass flask) was 9 mL/cm H₂O (Fig. 2).

The Fleisch-type, heating-optional pneumotachograph (3700, Hans Rudolph, Shawnee, Kansas) had a linear voltage signal over a range of flows (± 140 L/min) when assessed against a calibrating flow meter (VT Plus, Biotek, Winooski, Vermont). For each portion of the experiment the analog signal from the flow sensor was amplified, low-pass filtered (160 Hz), and digitally sampled at 500 Hz with a laptop computer and software (Labview 8.5, National Instruments, Austin, Texas) engineered to generate a raw flow/pressure signal (analog V_T). Each reported V_T reflected the mean of the inspiratory and expiratory V_T , or positive and negative deflections of the high-frequency analog signal, over a 2-second epoch. All data were continuously recorded and tabulated on a computer.

As an accepted standard comparator to analog V_T , a pressure-integrated high-frequency volume measurement (or adiabatic V_T) was derived from a transducer mounted within the glass-bottle apparatus. An implicit assumption of this protocol, and of preceding high-frequency flow-sensor validation studies, was that in vitro gas flow conformed to adiabatic properties.²⁰ Following Boyle's law, adiabatic V_T was calculated by incorporating the high-frequency pressure amplitude into the adiabatic gas formula (see Equation 1). The (± 2 cm H₂O) pressure transducer and amplifier (1110 series pneumotachometer amplifier, Hans Rudolph, Shawnee, Kansas) had a flat-frequency response of at least 25 Hz and a linear pressure response to ± 110 cm H₂O. The pressure signal was similarly low-pass filtered (160 Hz) and sampled at 500 Hz.

$$\text{Adiabatic } V_T = V \cdot \Delta P / \gamma \cdot P_o \quad (1)$$

in which V is the volume of the glass flask, ΔP is the high-frequency pressure amplitude, γ is the heat-loss ratio (1.39 for oxygen, and 1.40 for dry air), and P_o is the barometric pressure.

Development of a Corrective Flow-Integration Algorithm

It has been consistently shown, regardless of flow-sensor construct, that raw analog V_T signals must be digitally integrated or corrected to account for changes in frequency-dependent effects.^{20,21} Integration was performed by applying a real-time correction factor to the analog V_T measurement at each frequency (1–12 Hz, in 1 Hz increments). The more accurate and precise calibrated V_T (henceforth known as the corrected V_T or high-frequency V_T) was a derivative of the product of analog V_T and the ratio of analog V_T to adiabatic V_T measured during baseline experiments (described below).

High-Frequency Protocol

Low-frequency breath cycling was turned off, resulting in a sustained high-frequency-only waveform. Calibrating baseline or default ventilator settings were performed at: 4–12 Hz, mean airway pressure (P_{aw}) setting of 20 cm H₂O, F_{IO_2} of 0.21, and a fixed inspiratory/expiratory ratio (high-frequency I:E) of 1:1, with an 8-mm ETT. As previously noted, analog V_T and adiabatic V_T results from the latter experiments were used to derive a corrected, frequency-specific V_T or high-frequency V_T . We then ascertained the magnitude of error in the corrected flow signal caused by changes in gas content, airway caliber, and/or physiologic conditions. The sensor was assessed, without further signal adjustment, across a range of frequencies (4–12 Hz),

P_{aw} (10, 20, 30 cm H₂O), and F_{IO_2} (0.21, 0.50, and 1.0), as well as during active heating (gas temperature of 32°C), heating and humidification (gas temperature of 32°C, 70% relative humidity), with 6, 7, and 8-mm inner-diameter ETTs, and at a high-frequency I:E of 1:2. The high-frequency protocol included a total of 63 mean high-frequency V_T measurements.

Flow Sensor Dead-Space Effect

In order to quantify flow-sensor-imposed dead space, adiabatic V_T was measured during the same high-frequency protocol experiments, with and without the flow sensor in line.

Ventilator and Mechanical Lung Setup: Low-Frequency Tidal Volume Measurement

The previously described flow sensor and computer arrangement was used to measure and analyze low-frequency V_T . Given the absence of a linear inspiratory flow, the low-frequency algorithm consisted of summing the difference between individual inspiratory and expiratory high-frequency V_T over the time interval spanning end-exhalation to end-inhalation, to produce the flow-sensor-derived low-frequency V_T .

The low-frequency V_T comparator (test-lung V_T) was derived from a mechanical test lung (5600i, Michigan Instruments, Grand Rapids, Michigan) calibrated per the manufacturer's instructions (see Fig. 2). A mechanical test lung was used for 2 reasons. First, it permitted one to examine whether glass-model-derived calibration could be extrapolated to other compliance/resistance conditions. Mechanical lung compliance and resistance could also be adjusted to more closely model physiologic conditions. Second, by studying HFPV under modeled physiologic conditions, one could comprehend potential test-lung V_T behavior in the clinical setting. Test-lung compliance, validated at the airway pressures utilized for the study, was set to model ALI-like conditions (40 mL/cm H₂O). Airway resistance was 5 cm H₂O/L/s. The test lung included an embedded pressure transducer to obtain adiabatically-derived V_T (manufacturer-recommended test-lung-specific software was used for measurement of test-lung V_T [Pneuvue 5600i software, Michigan Instruments, Grand Rapids, Michigan). Notably, no test-lung- V_T -based calibration adjustment of the low-frequency V_T signal was required to enhance low-frequency flow sensor accuracy.

For the low-frequency protocol, conditions identical to the high-frequency protocol were explored with an additional array of low-frequency inspiratory time/respiratory rate combinations (10 breaths/min with an inspiratory time 1, 2, or 3 s, or 20 breaths/min with an inspiratory time of 1 or 2 s) and applied PEEP of 5 or 10 cm H₂O). Each

experiment collected and averaged data over 10 consecutive low-frequency breaths. The low-frequency protocol included a total of 105 mean low-frequency V_T measurements.

Statistical Analysis

For both the high-frequency and low-frequency experiments the comparison between high-frequency V_T and adiabatic V_T , and flow-sensor-derived low-frequency V_T and adiabatically derived low-frequency V_T , respectively, was performed with Bland-Altman analysis, with 95% confidence intervals (CIs).²⁵ As error in V_T may increase in proportion to V_T size, the percent error (% error) (see Equation 2), as opposed to the absolute difference, was used.

$$\% \text{ error} = 100\% \cdot (V_{TX} - \text{adiabatic } V_{Ty}) / V_T \text{ mean} \quad (2)$$

in which x is either the high-frequency V_T for the high-frequency protocol or the flow-sensor-derived low-frequency V_T for the low-frequency protocol, and y is either the adiabatic V_T for the high-frequency, or the adiabatically derived low-frequency V_T for the low-frequency protocol.

The study also included a simple descriptive analysis (difference in the means at each frequency) of the effects of ventilator settings (eg, frequency, P_{aw} , high-frequency I:E) and ETT diameter on adiabatically derived high-frequency V_T . Baseline or default settings served as a comparison for each change in frequency, unless explicitly stated otherwise.

Results

As anticipated, the raw analog V_T signals required integration or correction to account for changes in frequency-dependent effects. To illustrate, during initial high-frequency experiments, changes in frequency led to a systematic, linear, biasing effect on mean unadjusted analog V_T relative to mean adiabatic V_T (mean \pm SD difference $3.1 \pm 3.2\%$, 95% CI 1.9–4.3%).

Application of a real-time corrected V_T (high-frequency V_T) improved flow-sensor accuracy and precision, with a mean difference of $-0.2 \pm 1.8\%$ (95% CI -0.5% to 0.9%) (Fig. 3). Changes in mean P_{aw} , high-frequency I:E, and ETT size, or the application of heated and humidified gas did not diminish high-frequency V_T accuracy or precision (Table 1). However, an F_{IO_2} of 1.0 led to systematic error (mean error $9.2 \pm 4.5\%$, 95% CI 6.3–12.1%) and required an additional correction factor. For oxygen calibration purposes, the previously mentioned baseline ventilator settings were reexamined with an F_{IO_2} of 1.0. We then used

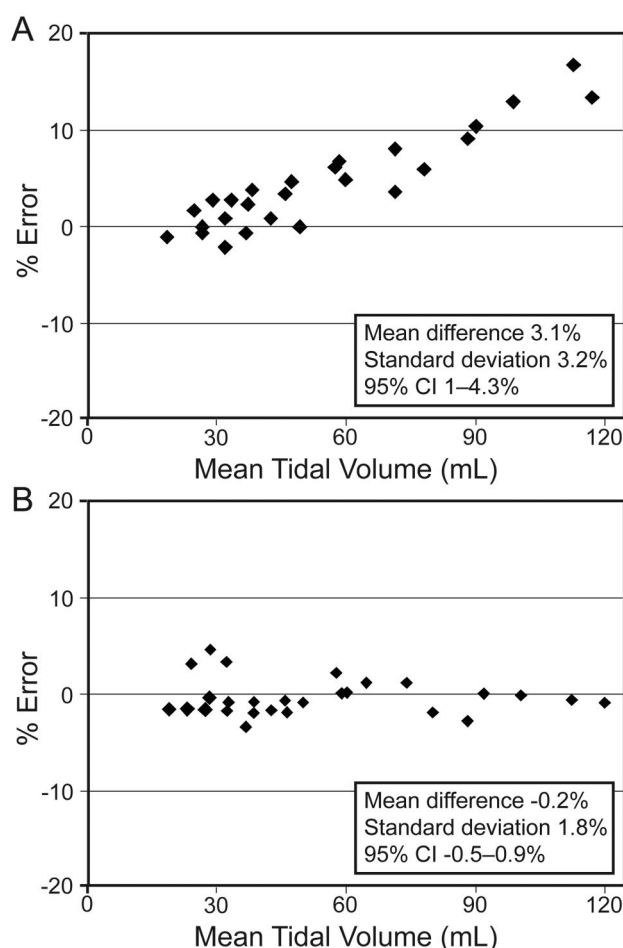


Fig. 3. A: Bland-Altman plot of the difference or percent error (% error, see Equation 2) between raw flow-sensor-derived high-frequency tidal volume and adiabatically derived high-frequency tidal volume, as a function of mean tidal volume. B: Plot of the difference between corrected high-frequency tidal volume. CI = confidence interval.

the analog V_T and adiabatic V_T results from the latter experiments to generate an $F_{IO_2} = 1.0$ specific corrected high-frequency V_T . This adjustment further enhanced flow-sensor accuracy (see Table 1).

Mean high-frequency V_T across the range of explored settings was 52.2 ± 27.1 mL (95% CI 41.9–62.5 mL). There was an exponential relationship between frequency and both mean adiabatic V_T and mean high-frequency V_T (see Equation 3 and Fig. 4).

$$\text{Adiabatic } V_T = 119.9e^{(-0.19\text{frequency})} \quad (3A)$$

$$\text{High-frequency } V_T = 118.27e^{(-0.17\text{frequency})} (r^2 \geq 0.99) \quad (3B)$$

Measurement of adiabatic V_T with and without the flow sensor in place disclosed a reduction in mean V_T of

Table 1. Mean Difference in High-Frequency V_T * Relative to Adiabatic V_T †

	Difference in High-Frequency V_T (mean \pm SD %)	95% CI
Mean Airway Pressure (cm H ₂ O)		
10	-0.8 ± 1.0	-1.4 to -0.2
20	-0.9 ± 1.4	-1.7 to 0.1
30	1.2 ± 2.2	-0.2 to 2.6
High-frequency I:E 1:1	-0.6 ± 2.0	-1.9 to 0.7
F _{IO₂}		
1.0	-0.6 ± 1.4	-1.5 to 0.3
0.5	-1.1 ± 2.4	-2.7 to 0.5
Heated gas	0.1 ± 2.3	-1.4 to 1.6
Heated and humidified gas	-0.1 ± 1.7	-1.2 to 1.0
ETT Inner Diameter (mm)		
6	0.3 ± 1.1	-0.4 to 1.0
7	-0.3 ± 1.7	-1.4 to 0.8

* High-frequency V_T = flow-sensor-derived high-frequency tidal volume.

† Adiabatic V_T = glass flask adiabatically derived high-frequency V_T .

I:E = inspiratory/expiratory ratio

ETT = endotracheal tube

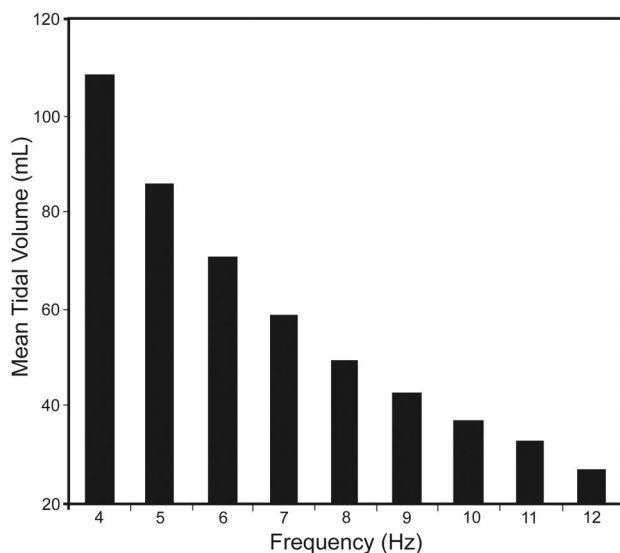


Fig. 4. Change in adiabatic tidal volume as a function of frequency (see text for discussion). For clarity, the graph demonstrates only adiabatic tidal volume at a single mean airway pressure setting of 20 cm H₂O, and a 21% oxygen concentration, with a fixed high-frequency inspiratory/expiratory ratio of 1:1.

-3.6 ± 2.7 mL (95% CI -1.6 to -5.6 mL) or a mean difference of $-5.7 \pm 4.3\%$ (95% CI -1.5% to -9.9%). Mean adiabatic V_T magnitude varied with changes in frequency, high-frequency I:E, ETT dimension, and mean P_{aw} (Table 2).

Flow sensor performance during low-frequency ventilation was accurate irrespective of inspiratory time and

Table 2. Changes in Adiabatic V_T *

	Difference in Adiabatic V_T (mean \pm SD %)	95% CI
↑ frequency by 1 Hz	-10.4 ± 7.4	-5.6 to -15.2
Δ ETT (from 8 to 7 mm)	-22.8 ± 1.3	-21.9 to -23.7
Δ ETT (from 8 to 6 mm)	-37.5 ± 1.5	-36.5 to -38.5
Δ high-frequency I:E (from 1:1 to 1:2)	-26.6 ± 4.9	-23.4 to -29.8
ΔP_{aw} (from 10 to 20 cm H ₂ O)	23.3 ± 9.6	13.7 to 29.6
ΔP_{aw} (from 20 to 30 cm H ₂ O)	-9.2 ± 9.6	-2.9 to -15.5

* At frequency range 4–12 Hz and various ventilator settings and endotracheal tube (ETT) diameters. The baseline, default settings (see Methods section) served as the comparison for each frequency change, unless explicitly stated otherwise.

Adiabatic V_T = glass flask adiabatically derived high-frequency V_T

I:E = inspiratory/expiratory ratio

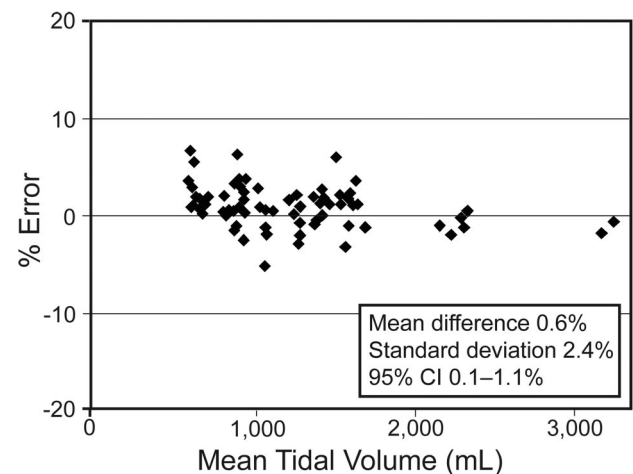


Fig. 5. Bland-Altman plot of the difference or percent error (% error, see Equation 2) between flow-sensor-derived low-frequency tidal volume (V_T) and adiabatically derived low-frequency V_T as a function of mean V_T during application of the flow-integration algorithm. Mean tidal volume = [(flow-sensor-derived low-frequency V_T + adiabatically derived low-frequency V_T)/2]. CI = confidence interval.

respiratory rate combination (mean difference $0.6 \pm 2.4\%$, 95% CI 0.1–1.1%) (Fig. 5) or change in high-frequency I:E, heated and humidified gas flow, oxygen content, applied PEEP setting, or ETT diameter (Table 3). Extended experiments (at a fixed high-frequency rate of 6 Hz and mean P_{aw} of 20 cm H₂O) revealed the flow sensor remained accurate during broader changes in airway resistance (5–15 cm H₂O/L/s) and compliance conditions (10–40 mL/cm H₂O) (data not shown). Using the studied range of HFPV settings resulted in low-frequency V_T extending from 607 mL to 3,452 mL (mean V_T $1,337 \pm 700$ mL, 95% CI 1,175–1,499 mL) (see Fig. 5).

Discussion

This study represents the first effort to provide an accurate and precise measurement of 2 separate HFPV gas

Table 3. Mean Difference in High-Frequency V_T * Relative to Test-Lung V_T †

	Difference in High-Frequency V_T (mean \pm SD %)	95% CI
High-frequency I:E 1:1	-0.3 ± 0.6	-0.7 to 0.1
F_{IO_2} 1.0	0.4 ± 0.7	-0.1 to 0.9
Heated and humidified gas	-0.7 ± 2.0	-2.0 to 0.6
6-mm ETT	0.6 ± 2.1	-0.8 to 2.0
Applied PEEP (cm H_2O)		
5	-0.2 ± 0.9	-0.8 to 0.4
10	-0.8 ± 1.4	-1.7 to 0.1

* High-frequency V_T = flow-sensor-derived high-frequency tidal volume.† Test-lung V_T = mechanical lung adiabatically derived low-frequency V_T .

I:E = inspiratory/expiratory ratio

ETT = endotracheal tube

 F_{IO_2} = fraction of inspired oxygen

flow patterns in real time. A simple corrective algorithm for adjusting the analog flow signal proved exact across the studied range of frequencies, mean P_{aw} , high-frequency I:E ratios, F_{IO_2} , and heated and humidified gas flows (see Tables 1 and 3 and Figs. 3 and 5). Moreover, flow-sensor accuracy was comparable to that achieved by flow sensors validated for use with other modes of high-frequency ventilation.¹⁸⁻²¹ Taken at face value, the use of pneumotachography for high-frequency flow analysis is a reliable and time-tested approach, and thus there is no novelty to our pneumotachograph validation. However, in the midst of performing a flow-sensor validation protocol specific to this dual-frequency mode of mechanical ventilation came several new discoveries and concerns regarding HFPV-administered high-frequency and low-frequency V_T , respectively.

As with other modes of high-frequency ventilation, an increase in ETT diameter and I:E or a reduction in high-frequency rate amplified high-frequency V_T (see Table 2).^{21,26,27} Surprisingly, there appeared to be a bell-shaped response to mean P_{aw} -specific V_T responses. At mean P_{aw} settings exceeding 20 cm H_2O (going from 20 to 30 cm H_2O) a reduction in mean high-frequency V_T was noted ($-9.2 \pm 9.6\%$, 95% CI -2.9 to -15.5%). The origin of the latter finding is unclear but may be a consequence of high- P_{aw} -induced venting of gas flow through pressure-release valves adjacent to the HFPV assembly.^{22,23}

Another original aspect to this study was the discovery that HFPV-administered high-frequency V_T carried an exponential frequency-dependent relationship (see Equation 3 and Fig. 4). Scalfaro et al revealed that high-frequency oscillatory ventilation also follows an exponential V_T reduction as frequency is increased.²⁰ HFPV may therefore draw upon the same or similar principles invoked for high-frequency oscillatory ventilation to augment patient oxygenation or ventilation. However, this comparison must

be examined in light of HFPV's continued use of low-frequency ventilation.

Our aforementioned concerns regarding previously volumetrically unmeasured HFPV appear well founded. Applying a representative range of HFPV settings during ALI-modeled conditions led to a mean V_T of $1,337 \pm 700$ mL (95% CI 1,175–1,499 mL). The latter results, extrapolated to a 70-kg patient, would correspond to a mean V_T of 19.1 mL/kg, which is far in excess of the 4–8 mL/kg recommended for patients with ALI.^{12,13} This revelation suggests that HFPV must be used with caution in patients with ALI, or, at the least, should be guided by real-time flow-sensor measurements to avoid the delivery of inordinate V_T . Continued exploration of V_T -driven HFPV algorithms may eventually advance HFPV into the conceptual framework of lung-protective ventilation.

The flow sensor system suffers from limitations. Improving upon analog signal accuracy required high-frequency-rate and oxygen-concentration-specific corrections. However, frequency and oxygen dependent modification were anticipated and remediable confounding elements.^{14-17,20,21} Though the sensor attachment carries an additional small dead space burden, this impediment can be overcome by compensatory measures such as lowering the high-frequency rate or augmenting the low-frequency minute ventilation.²¹ Application of bench-top findings to clinically relevant bedside use can also be challenging. Nevertheless, as part of an ongoing follow-on protocol, preliminary experience has shown that the flow sensor is amenable to near-automated “plug-and-play” adaptability, permitting clinicians the opportunity to make real-time ventilator adjustments based on flow sensor measurements. Indeed, clinical application of the flow sensor has confirmed the existence of previously unrecognized large V_T delivery during HFPV (unpublished observation). These findings have led to a marked change in how we approach HFPV programming.

Conclusions

A readily available pneumotachograph accurately and precisely gauged high-frequency and low-frequency V_T during HFPV. This early experience suggests that the device may be an agreeable substitute or supplement to current HFPV transducers. Notably, flow-sensor measurements have pinpointed that, in the setting of ALI, typical HFPV settings may deliver injurious V_T .

ACKNOWLEDGMENTS

Thanks to Erik C Osborn MD, Michelle Perello DO, and William H Gasaway, for their contributions to protocol design and manuscript editing, and to Cornelia Camerer and Meredith Pride for their invaluable research efforts.

REFERENCES

- Cioffi WG, Rue LW 3rd, Graves TA, McManus WF, Mason AD, Pruitt BA Jr. Prophylactic use of high-frequency percussive ventilation in patients with inhalation injury. *Ann Surg* 1991;213(6):575-582.
- Rue LW 3rd, Cioffi WG, Mason AD, McManus WF, Pruitt BA Jr. Improved survival of burned patients with inhalation injury. *Arch Surg* 1993;128(7):772-778.
- Reper P, Wibaux O, Van Laeke P, Vandeenen D, Duinslaeger L, Vanderkelen A. High frequency percussive and conventional ventilation after smoke inhalation: a randomized study. *Burns* 2002;28(5):503-508.
- Reper P, Van Bos R, Van Loey K, Van Laeke P, Vanderkelen A. High frequency percussive ventilation in burn patients: hemodynamics and gas exchange. *Burns* 2003;29(6):603-608.
- Hall JJ, Hunt JL, Arnoldo BD, Purdue GF. Use of high-frequency percussive ventilation in inhalation injuries. *J Burn Care Res* 2007;28(3):396-400.
- Velmahos GC, Chan LS, Tatevossian R, Cornwell EE 3rd, Dougherty WR, Escudero J, Demetriades D. High-frequency percussive ventilation improves oxygenation in patients with ARDS. *Chest* 1999;116(2):440-446.
- Paulson SM, Killyon GW, Barillo DJ. High-frequency percussive ventilation as a salvage modality in adult respiratory distress syndrome: a preliminary study. *Am Surg* 2002;68(10):854-856.
- Hurst JM, Branson RD, DeHaven CB. The role of high-frequency ventilation in post-traumatic respiratory insufficiency. *J Trauma* 1987;27(3):236-242.
- Hurst JM, Branson RD, Davis K, Barrette RR, Adams KS. Comparison of conventional mechanical ventilation and high-frequency ventilation. *Ann Surg* 1990;211(4):486-491.
- Eastman A, Holland D, Higgins J, Smith B, Delagarza J, Olson C, et al. High-frequency percussive ventilation improves oxygenation in trauma patients with acute respiratory distress syndrome: a retrospective review. *Am J Surg* 2006;192(2):191-195.
- Salim A, Martin M. High-frequency percussive ventilation. *Crit Care Med* 2005;33(3):S241-S245.
- NHLBI Acute Respiratory Distress Syndrome Network. Ventilation with lower tidal volumes as compared with traditional tidal volumes for acute respiratory distress syndrome. *N Engl J Med* 2000;342(18):1301-1308.
- Malhotra A. Low-tilal-volume ventilation in the acute respiratory distress syndrome. *N Engl J Med* 2007;357(11):1113-1120.
- Foitzik B, Schmalisch G, Wauer RR. Effect of physical properties of respiratory gas on pneumotachographic measurement of ventilation in newborn infants. *Biomed Tech* 1994;39(4):85-92.
- Jackson AC, Vinegar A. A technique for measuring frequency response of pressure, volume, and flow transducers. *J Appl Physiol* 1979;47(2):462-467.
- Finucane KE, Egan BA, Dawson SV. Linearity and frequency response of pneumotachographs. *J Appl Physiol* 1972;32(1):121-126.
- Francis G, Gelfand R, Peterson RE. Effects of gas density on the frequency response of gas filled pressure transducers. *J Appl Physiol* 1979;47(3):631-637.
- Courtney SE, Weber KR, Spohn WA, Malin SW, Bender CV, Gotshall RW. Measurement of tidal volume using a pneumotachometer during high-frequency oscillation. *Crit Care Med* 1990;18(6):651-653.
- Hoskyns EW, Milner AD, Hopkin IE. Measurement of tidal lung volumes in neonates during high-frequency oscillation. *J Biomed Eng* 1992;14(1):16-20.
- Scalfaro P, Pillow JJ, Sly PD, Cotting J. Reliable tidal volume estimates at the airway opening with an infant monitor during high-frequency oscillatory ventilation. *Crit Care Med* 2001;29(10):1925-1930.
- Hager DN, Fuld M, Kaczka DW, Fessler HE, Brower RG, Simon BA. Four methods of measuring tidal volume during high-frequency oscillatory ventilation. *Crit Care Med* 2006;34(3):751-757.
- Allan PF, Thurlby JR, Naworol GA. Measurement of pulsatile tidal volume, pressure amplitude, and gas flow during high-frequency percussive ventilation, with and without partial cuff deflation. *Respir Care* 2007;52(1):45-49.
- Allan PF, Naworol G. Corrective measures for compromised oxygen delivery during endotracheal tube cuff deflation with high-frequency percussive ventilation. *Respir Care* 2007;52(3):271-277.
- Allan PF, Hollingsworth MJ, Maniere GC, Rakofsky AK, Chung KK, Naworol GA et al. Airway humidification during high-frequency percussive ventilation. *Respir Care* 2009;54(3):350-358.
- Bland JM, Altman DG. Statistical methods for assessing agreement between two methods of clinical measurement. *Lancet* 1986;1(8476):307-310.
- Chan V, Greenough A, Milner AD. The effect of frequency and mean airway pressure on volume delivery during high-frequency oscillation. *Pediatr Pulmonol* 1993;15(3):183-186.
- Hager DN, Fessler HE, Kaczka DW, Shanholtz CB, Fuld MK, Simon BA, Brower RG. Tidal volume delivery during high-frequency oscillatory ventilation in adults with acute respiratory distress syndrome. *Crit Care Med* 2007;35(6):1522-1529.